

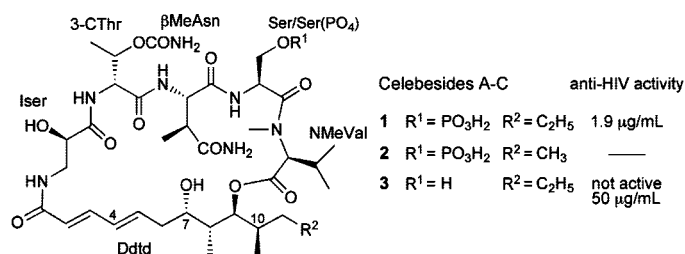
Celebesides A–C and Theopapuamides B–D, Depsipeptides from an Indonesian Sponge That Inhibit HIV-1 Entry

Alberto Plaza,[†] Giuseppe Bifulco,[‡] Jessica L. Keffer,[†] John R. Lloyd,[†] Heather L. Baker,[†] and Carole A. Bewley^{*,†}

Laboratory of Bioorganic Chemistry, National Institute of Diabetes and Digestive and Kidney Diseases, National Institutes of Health, Bethesda, Maryland 20892-0820, and Dipartimento di Scienze Farmaceutiche, University of Salerno, Via Ponte Don Melillo, 84084 Fisciano, Salerno, Italy

caroleb@mail.nih.gov

Received October 7, 2008



Six new depsipeptides belonging to two different structural classes, termed celebesides A–C and theopapuamides B–D, have been isolated from the marine sponge *Siliquariaspongia mirabilis*. Their structures were determined using extensive 2D NMR and ESI-MS/MS techniques. Celebesides are unusual cyclic depsipeptides that comprise a polyketide moiety and five amino acid residues, including an uncommon 3-carbamoyl threonine, and a phosphoserine residue in celebesides A and B. Theopapuamides B–D are undeca-peptides with an N-terminal fatty acid moiety containing two previously unreported amino acids, 3-acetamido-2-aminopropanoic acid and 4-amino-2,3-dihydroxy-5-methylhexanoic acid. The relative configuration of the polyketide moiety in celebesides was resolved by *J*-based analysis and quantum mechanical calculations, the results of which were self-consistent. Celebeside A neutralized HIV-1 in a single-round infectivity assay with an IC₅₀ value of 1.9 ± 0.4 μg/mL while the nonphosphorylated analog celebeside C was inactive at concentrations as high as 50 μg/mL. Theopapuamides A–C showed cytotoxicity against human colon carcinoma (HCT-116) cells with IC₅₀ values between 2.1 and 4.0 μg/mL and exhibited strong antifungal activity against wildtype and amphotericin B-resistant strains of *Candida albicans* at loads of 1–5 μg/disk.

Introduction

Lithistid demosponges are an abundant source of structurally diverse and biologically active natural products, which may be in part due to the biosynthetic capacity of the bacteria that they host.^{1,2} In particular, marine sponges belonging to the Theonellidae family have yielded a number of unique compounds² with a broad spectrum of biological activities, including antifungal³ and cancer cell growth inhibitors.^{4,3d} Among this

family, the chemistry of the genus *Siliquariaspongia* has been little studied.⁵ Recently, we reported the structures of a potent

* To whom correspondence should be addressed. Tel: (301) 594-5187. Fax: (301) 480-3447.

[†] National Institute of Diabetes and Digestive and Kidney Diseases.

[‡] University of Salerno.

(1) Bewley, C. A.; Faulkner, D. J. *Angew. Chem., Int. Ed. Engl.* **1998**, *37*, 2162.

(2) Matsunaga, S.; Fusetani, N. *Curr. Org. Chem.* **2003**, *7*, 945.

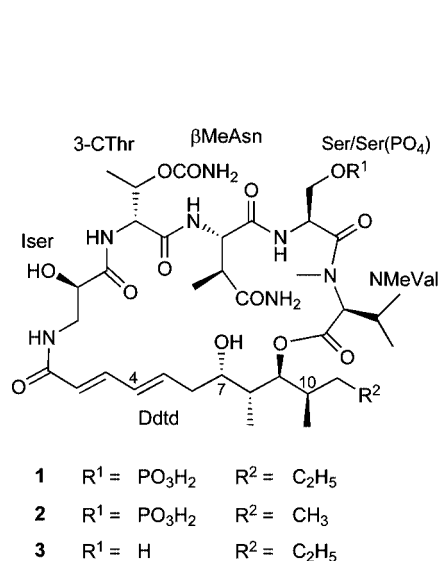
(3) (a) Matsunaga, S.; Fusetani, N.; Kato, Y.; Hirota, H. *J. Am. Chem. Soc.* **1991**, *113*, 9690. (b) Matsunaga, S.; Fusetani, N.; Hashimoto, K.; Walchli, M. *J. Am. Chem. Soc.* **1989**, *111*, 2582. (c) Bewley, C. A.; Faulkner, D. J. *J. Org. Chem.* **1994**, *59*, 4849. (d) Youssef, D. T. A.; Mooberry, S. L. *J. Nat. Prod.* **2006**, *69*, 154.

(4) (a) Kashman, Y.; Carmely, S. *Tetrahedron Lett.* **1985**, *26*, 511. (b) Kobayashi, M.; Tanaka, J.; Katori, T.; Matsuura, M.; Kitagawa, I. *Tetrahedron Lett.* **1989**, *22*, 2963. (c) Kitagawa, I.; Kobayashi, M.; Katori, T.; Yamashita, M.; Tanaka, J.; Doi, M.; Ishida, T. *J. Am. Chem. Soc.* **1990**, *112*, 3710. (d) Doi, M.; Ishida, T.; Kobayashi, M.; Kitagawa, I. *J. Org. Chem.* **1991**, *56*, 3629. (e) Hamada, T.; Matsunaga, S.; Yano, G.; Fusetani, N. *J. Am. Chem. Soc.* **2005**, *127*, 110.

(5) (a) Sata, N. U.; Matsunaga, S.; Fusetani, N.; van Soest, R. W. M. *J. Nat. Prod.* **1999**, *62*, 969. (b) Sata, N. U.; Wada, S.-i.; Matsunaga, S.; Watabe, S.; van Soest, R. W. M.; Fusetani, N. *J. Org. Chem.* **1999**, *64*, 2331.

(6) Plaza, A.; Baker, H. L.; Bewley, C. A. *J. Nat. Prod.* **2008**, *71*, 473.

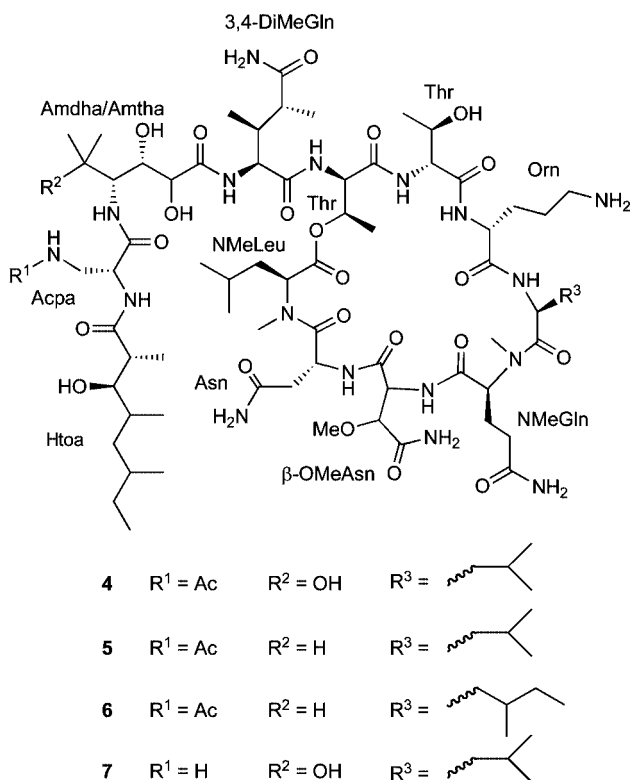
antitumor macrolide, mirabalin,⁶ and several glycosylated depsipeptides, mirabamides A–D, that inhibit HIV-1 fusion,⁷ from a *Siliquariaspongia mirabilis* sample collected in Chuuk. As part of our ongoing research on new bioactive natural products from marine organisms, we identified an aqueous extract of an Indonesian collection of *S. mirabilis* that showed activity in HIV-1 neutralization, antifungal, and cytotoxicity assays. Bioassay-guided fractionation yielded a Sephadex fraction containing six new depsipeptides of two different structural classes, termed celebesides A–C (**1–3**), and theopapuamides B–D (**4–6**). The previously reported theopapuamide (**7**)⁸ was also isolated from the same fraction. The structures of **1–6** were elucidated by extensive spectroscopic methods including 1D and 2D NMR experiments as well as ESI-MS analysis. The absolute configurations of the amino acids were determined by LCMS (advanced Marfey's method)⁹ and chiral HPLC. The relative configurations of the chiral centers of the polyketide residues were established by combined analysis of homonuclear (H–H) and heteronuclear (C–H)^{2,3} *J* couplings, ROE data, and quantum mechanical calculations.



Results and Discussion

The HR-ESI-MS of celebeside A (**1**) showed a major ion peak at *m/z* 892.4054 [M + H]⁺ corresponding to a molecular formula of C₃₇H₆₂N₇O₁₆P (calcd for C₃₇H₆₃N₇O₁₆P, 892.40689) and suggesting the presence of a phosphate group. The ¹H NMR spectrum of **1** exhibited signals characteristic of a peptide

containing a polyketide section including six exchangeable NH protons from δ 6.68 to 8.14; one methyl amide at δ 3.05 (3H, s); six methyl doublets at δ 0.74 (3H, d, *J* = 6.6 Hz), 0.794 (3H, d, *J* = 7.0 Hz), 0.796 (3H, d, *J* = 6.0 Hz), 0.93 (3H, d, *J* = 6.4 Hz), 1.10 (3H, d, *J* = 7.1 Hz), and 1.17 (3H, d, *J* = 6.4 Hz); and one methyl triplet at δ 0.82 (3H, t, *J* = 7.1 Hz). Signals corresponding to four olefinic protons at δ 6.00 (1H, d, *J* = 15.5 Hz), 6.05 (1H, dd, *J* = 15.3, 6.6), 6.23 (1H, dd, *J* = 15.3, 11.1 Hz), and 7.06 (1H, dd, *J* = 15.5, 11.1 Hz) were present in the downfield region of the spectrum. The HSQC spectrum clearly showed that the four methines from δ 4.47 to 4.92, and the methylene at δ 3.55 and 3.41 were correlated to five carbons at δ 43.9 to 63.0, indicating the presence of five amino acid residues (see Table 1). This evidence in combination with the DQF-COSY, 2D-HOHAHA, and HMBC correlations allowed us to establish the presence of *N*-methylvaline (NMeVal), serine, β -methylasparagine (β MeAsn), threonine, and isoserine (Iser). The downfield chemical shift of the threonine β -oxymethine proton at δ 5.01 and its HMBC correlation to a carbonyl resonance at δ 157.8 indicated an ester linkage of the threonine



residue to a carbamic acid.¹⁰ In similar fashion, phosphorylation of the serine residue (pSer) was deduced from the downfield chemical shifts observed for the β -oxymethylene of serine (δ_{H} 3.85 and 3.95, δ_{C} 65.2) in the HSQC spectrum. Furthermore, these results were corroborated by ESI-MS/MS analysis. The daughter ion spectrum of the major ion at *m/z* 914 [M + Na]⁺ displayed fragment ions at *m/z* 853 [M + Na - 61]⁺ and *m/z* 816 [M + Na - 98]⁺ corresponding to the neutral loss of a carbamic acid residue and a phosphate group, respectively. To our knowledge, this is the first occurrence of a 3-carbamoyl threonine (3-CThr) or a phosphorylated serine residue in a marine natural product.

(7) Plaza, A.; Gustchina, E.; Baker, H. L.; Kelly, M.; Bewley, C. A. *J. Nat. Prod.* **2007**, *70*, 1753.

(8) Ratnayake, A. S.; Bugni, T. S.; Feng, X.; Harper, M. K.; Skalicky, J. J.; Mohammed, K. A.; Andjelic, C. D.; Barrows, L. R.; Ireland, C. M. *J. Nat. Prod.* **2006**, *69*, 1582.

(9) (a) Fujii, K.; Ikai, Y.; Oka, H.; Suzuki, M.; Harada, K.-I. *Anal. Chem.* **1997**, *69*, 5146. (b) Fujii, K.; Ikai, Y.; Mayumi, T.; Oka, H.; Suzuki, M.; Harada, K.-I. *Anal. Chem.* **1997**, *69*, 3346.

(10) Bui, H. T. N.; Jansen, R.; Pham, H. T. L.; Mundt, S. *J. Nat. Prod.* **2007**, *70*, 499.

(11) Goldberg, J.; Huang, H. B.; Kwon, Y. G.; Greengard, P.; Nairn, A. C.; Kuriyan, J. *Nature* **1995**, *376*, 745.

TABLE 1. NMR Spectroscopic Data for Celebeside A (1) (CD₃CN–D₂O 5:1)

	δ_C^a	δ_H^b (J in Hz)	HMBC ^c	ROESY ^d
	Iser			
1	174.9			
2	70.4	4.25 dd (7.8, 3.1)	1, 3	3a, 1 _{Thr}
3a	43.9	3.55 m	1, 2, 1 _{Dtdt}	NH
3b		3.41 m	1, 2, 1 _{Dtdt}	NH
NH		7.98 br t (5.3)		2, 3, 2 _{Dtdt} , 3 _{Dtdt}
	3-CThr			
1	171.2			
2	57.7	4.62 dd (8.0, 4.5)	1, 3, 4, 1 _{Iser}	3, 4, NH, NH _{βMeAsn}
3	71.0	5.01 m	1, 2, 4, CO _{carbamic acid}	2, 4
Me-3	16.9	1.17 d (6.4)	2, 3	2, 4
4	157.8			
NH ₂ -4		Na		
NH		8.02 d (8.0)		2, 3, 4, 2 _{Iser}
	β MeAsn			
1	171.6			
2	56.3	4.47 dd (8.2, 5.1)	1, 3, 4, β Me, 1 _{Thr}	3, β Me, NH, NH _{Ser}
3	41.0	3.09 m	2, 4, β Me	2, β Me, NH ₂ -4
4	178.9			
β Me	15.5	1.10 d (7.1)	2, 3, 4	2, 3, NH, NH ₂ -4
NH		8.14 (8.2)		1, β Me, 2 _{Thr} , 3 _{Thr}
NH ₂ -4		6.68		3
		7.26		3, β Me
	pSer			
1	171.2			
2	51.4	4.92 m	1, 3, 1 _{βMeAsn}	3, NH, NMe _{NMeVal}
3 ^a	65.2	3.95 dd (9.6, 18.0)	1, 2	2, NH, 3 _{Dtdt} , 4 _{Dtdt} , 5 _{Dtdt}
3b		3.85 m	1	2, NH, 3 _{Dtdt} , 4 _{Dtdt} , 5 _{Dtdt}
NH		7.85 d (4.6)		2, 3, 2 _{βMeAsn}
	NMeVal			
1	171.3			
2	63.0	4.70 d (10.7)	1, 4, 5, NMe, 1 _{pSer}	4, 5, NMe, 7 _{Dtdt}
3	27.7	2.15 m	1, 2, 4, 5	4, 5, NMe
4	18.7	0.74 d (6.4)	2, 3, 5	2, 3, NMe
5	19.7	0.93 d (6.4)	2, 3, 4	2, 3, NMe
NMe	31.7	3.05 s	2, 1 _{pSer}	2, 3, 4, 5, 2 _{Ser}
	Dtdt			
1	169.5			
2	123.5	6.00 d (15.5)	1, 3, 4, 5	NH _{Iser}
3	141.6	7.06 dd (15.5, 11.1)	1, 2, 4, 5	5, NH _{Iser}
4	131.4	6.23 dd (15.3, 11.1)	2, 3, 5, 6, 7	6, 7, 8, Me-8, ^e 3 _{Ser} , NMe _{NMeVal}
5	140.2	6.05 dd (15.3, 6.6)	3, 4, 6, 7	6, 7, 8, Me-8, ^e 3 _{Ser} , NMe _{NMeVal}
6a	38.6	2.34 td (13.9, 6.6)	4, 5, 7, 8	4, 5, 7, Me-8 ^e
6b		2.20 td (13.9, 6.6)	4, 5, 7, 8	4, 5, 7, Me-8 ^e
7	70.6	3.33 t (7.4)	5, 6, 8, 9, Me-8	4, 5, 6, 8, 9, 2 _{NMeVal}
8	38.5	1.70 m	9, Me-8	4, 5, 7, 9, Me-8, ^e Me-10 ^e
9	78.7	5.00 dd (10.6, 1.1)	6, 7, 10, 11 Me-8, Me-10	7, 8, 10, ^e 11, ^e Me-8 ^e
10	34.3	1.76 m	11, 12, Me-10	9, 12 ^e
11a	37.5	1.18 m	10, 12, Me-10	9 ^e
11b		1.08 m	10, 12Me-10	9 ^e
12a	21.0	1.30 m	10, 11, 13	9, ^e 10 ^e
12 b		1.19 m		9, ^e 10 ^e
13	14.5	0.82 t (7.1)	11, 12	
Me-8	9.00	0.794 d (7.0)	7, 8, 9	7, ^e 8, ^e 9, ^e 10 ^e
Me-10	12.9	0.796 d (6.0)	9, 10, 11	8, ^e 9, ^e 10 ^e

^a Recorded at 500 MHz; referenced to residual CD₃CN at δ 1.93 ppm. ^b Recorded at 125 MHz; referenced to residual CD₃CN at δ 117.7 ppm. ^c Proton showing HMBC correlation to indicated carbon (CD₃CN–D₂O 5:1). ^d Proton showing ROESY correlation to indicated proton (CD₃CN–H₂O 5:1). ^e ROE correlation obtained from the HSQC-ROESY spectrum (CD₃CN–D₂O 5:1).

The structure of the polyketide residue was deduced as follows. A conjugated diene spin system (δ_{H-2} 6.00, δ_{C-2} 123.5, δ_{H-3} 7.06, δ_{C-3} 141.6, δ_{H-4} 6.23, δ_{C-4} 131.4, δ_{H-5} 6.05, δ_{C-5} 140.2) assigned from HSQC-TOCSY and COSY correlations was linked to a carbonyl group by HMBC correlations from the H-2 and H-3 protons to the carbon resonance at δ_C 169.5 (C-1). HSQC-TOCSY and COSY correlations extended the diene spin system to a sequential allylic methylene (δ_{H-6} 2.34, 2.20, δ_{C-6} 38.6), an oxymethine (δ_{H-7} 3.33, δ_{C-7} 70.6), a methine (δ_{H-8} 1.70, δ_{C-8} 38.5), and additional oxymethine group (δ_{H-9} 5.00, δ_{C-9} 78.7). Finally, key long-range correlations from the methyl

protons at δ 0.794 (Me-8) to the carbon resonances at δ 70.6, 38.5, and 78.7; from the methyl protons at δ 0.796 (Me-10) to the carbon resonances at δ 78.7, 34.3 (C-10), and 37.5 (C-11); and from the secondary methyl at δ 0.82 (Me-13) to the carbon resonances at δ 21.0 and 37.5 allowed complete assembly of the polyketide residue. On the basis of this information the structure of the polyketide residue was established as 7,9-dihydroxy-8,10-dimethyltrideca-2,4-dienoic acid (Dtdt).

The complete sequence of **1** was obtained from HMBC and ROESY correlations. Long-range correlations between α -protons to carbonyl carbons of adjacent amino acids and ROE correla-

tions from α -protons to NH protons of adjacent amino acids allowed us to establish the following sequence: Iser-3-CThr- β MeAsn-pSer-NMeVal (see Table 1). Moreover, connectivity of the Ddtd unit to the N-terminus of Iser was indicated from an HMBC correlation between the Iser α -methylene protons (δ 3.55 and 3.41) and the carbonyl at δ 169.5 (C-1_{Ddtd}). Finally, the downfield chemical shift of the Ddtd oxymethine proton at δ 5.00 (H-9_{Ddtd}) suggested an ester linkage at this position, which was confirmed by an HMBC correlation between H-9_{Ddtd} and the carbonyl carbon of NMeVal (δ 171.3), thereby completing the structure of **1** as a 26-membered ring. Tandem mass spectrometry provided further evidence to support the structure of **1**. MS³ fragmentation of the daughter ion at m/z 853 [M + Na – NH₂CO₂H]⁺ displayed fragment ions at m/z 755 [M + Na – NH₂CO₂H – H₃PO₄]⁺, and m/z 740 [M + Na – NH₂CO₂HNa – NMeVal]⁺. Successively, MS⁴ fragmentation of the ion peak at m/z 755 gave fragments at m/z 642 [M + Na – NH₂CO₂HNa – H₃PO₄Na – NMeVal]⁺, m/z 573 [M + Na – NMeVal-Pser]⁺, and m/z 390 [M + Na – NH₂CO₂HNa – H₃PO₄Na – NMeVal-Ddtd]⁺. Thus, the MSⁿ fragmentation patterns were in complete agreement with the structure of **1** determined by NMR.

The absolute configurations of L-NMeVal, L-Ser, D-3-CThr, and D-Iser residues were assigned by MS-detected chromatographic comparison of the acid hydrolysate (5 N HCl, 90 °C, 16 h) of **1** with L-FDLA (1-fluoro-2,4-dinitrophenyl-5-L-leucinamide)⁹ and D-FDLA derivatives of amino acid standards. The absolute configuration of β MeAsn was also established by this method owing to the report by Fujii et al.^{9a} that the L-FDLA derivative of β MeAsn elutes before the D-FDLA derivative. As detected by LC–MS (reconstructed ion chromatogram, m/z 440 [MNa – H][–]), L/D-FDLA derivatives of β MeAsn of **1** eluted at 20.9 and 22.1 min while the L-FDLA derivative eluted at 20.9 min, thus establishing the configuration of β MeAsn as L. To distinguish between *erythro* and *threo* configurations, L-FDLA and D-FDLA derivatives of β MeAsn in **1** and in an authentic sample of microcystin LR, shown by X-ray crystallography to contain *erythro*-D- β MeAsn,¹¹ were compared. LC–MS analysis showed the D-FDLA derivative of **1** to coelute with the L-FDLA derivative of microcystin; thus celebeside A must contain *erythro*-L- β MeAsn. Further confirmation of the *erythro* configuration was provided from Murata's *J*-based configurational analysis.¹² The combination of a medium vicinal coupling constant between H-3 _{β MeAsn} and H-2 _{β MeAsn} (5.5 Hz), a small ³*J*_{H–C} for H-2 _{β MeAsn}/ β Me β MeAsn (2.2 Hz), and a medium ²*J*_{H–C} for H-3 _{β MeAsn}/C-2 _{β MeAsn} (–3.0 Hz) is indicative of an *erythro* (2*S*,3*R*) configuration at C-2/C-3.

Several techniques were used to establish the configurations of the Ddtd unit. The *E* geometries of the Δ^{2-3} and Δ^{4-5} olefins were apparent from the large ³*J*_{H–H} values of 15.5 and 15.3 Hz between H-2_{Ddtd}/H-3_{Ddtd} and H-4_{Ddtd}/H-5_{Ddtd}, respectively. The relative configurations of the chiral centers at C-7, C-8, C-9, and C-10 in Ddtd were determined by a combination of *J*-based configurational analysis,¹² and quantum mechanical calculations of the homonuclear and heteronuclear *J*-coupling values. Experimental data including ³*J*_{H–H} (¹H NMR and E.COSY¹³) and ^{2,3}*J*_{C–H} couplings and ROEs were compared to those predicted for all possible staggered rotamers (Figure 1). Due to the complex multiplicity and small homonuclear coupling

constants of the methine protons H-8_{Ddtd} and H-10_{Ddtd}, heteronuclear coupling constants were accurately measured from 2D NMR experiments including HETLOC,¹⁴ HSQMBC,¹⁵ and constant time *J*-resolved HMBC¹⁶ experiments, and ROE correlations were obtained from ROESY and HSQC-ROESY¹⁷ experiments. All experiments were recorded on samples dissolved in a mixture of 5:1 CD₃CN–D₂O at 298 K. A small ³*J*_{H–H} of 1.0 Hz between H-7_{Ddtd} and H-8_{Ddtd} indicated a *gauche* configuration between these protons, and a small heteronuclear ³*J*_{C–H} of 3.1 Hz indicated a *gauche* configuration between H-7_{Ddtd} and C-9_{Ddtd}. Together, these values rule out models **A1**, **A2**, **A4**, and **A6** (Figure 1a). Additionally, respective ³*J*_{C–H} values of 2.6 and 5.5 Hz for H-8_{Ddtd}/C-6_{Ddtd} and H-7_{Ddtd}/Me-8_{Ddtd} excluded rotamer **A5** indicating the correct conformation to be that depicted in **A3**. Strong ROEs between H-7_{Ddtd} and H-8_{Ddtd}, H-7_{Ddtd} and H-9_{Ddtd}, and H-6_{Ddtd} and Me-8_{Ddtd} corroborated this result and established a *syn* configuration for C-7_{Ddtd} and C-8_{Ddtd}. The *anti* configuration between Me-8_{Ddtd} and the hydroxyl group at C-9_{Ddtd}, corresponding to rotamer **B4**, was deduced from the large coupling constant between H-8_{Ddtd} and H-9_{Ddtd} (10.6 Hz) and strong HSQC-ROESY correlations between Me-8_{Ddtd} and H-10_{Ddtd} and Me-8_{Ddtd} and H-9_{Ddtd} (Figure 1b). The small ³*J*_{H–H} of 1.1 Hz between H-9_{Ddtd} and H-10_{Ddtd} (Figure 1c) indicated a *gauche* configuration between these protons, while a small heteronuclear coupling of ²*J*_{H10–C9} = 1.3 Hz obtained from the G-BIRD-HSQMBC spectrum indicated an *anti* orientation between H-10_{Ddtd} and the hydroxyl group at C-9_{Ddtd}. Taken together, these data rule out rotamers **C2**–**C5** (Figure 1c). The relatively large ³*J*_{Me10–H9} value of 5.3 Hz suggested an *anti* configuration between H-9_{Ddtd} and Me-10_{Ddtd} and further excluded model **C6**. Therefore, the relative configuration for C-9_{Ddtd}/C-10_{Ddtd} was established as *anti*. This result was supported by ROE correlations between H-9_{Ddtd} and H-10_{Ddtd} and H-9_{Ddtd} and H-11_{Ddtd}, and a strong HSQC-ROESY correlation between H-8_{Ddtd} and Me-10_{Ddtd}. On the basis of the results obtained by using Murata's method, the relative configuration of the chiral centers in Ddtd was established as 7*S**, 8*R**, 9*S**, 10*R**.

Strictly speaking, the NMR *J*-based analysis is applicable to staggered rotamers within acyclic carbon chains.¹⁸ As Ddtd is located within a macrocycle, we sought to corroborate the relative configuration of its chiral centers by using an integrated NMR-quantum mechanical approach that relies on the comparison between calculated and experimental ³*J*_{H–H} and ^{2,3}*J*_{C–H} values.¹⁹ This approach is particularly appropriate in cases where experimentally determined coupling constants fall between the ranges qualitatively classified as “large” or “small”. While the ¹H resolution and relatively large range (0–12 Hz) of homonuclear three-bond coupling constants facilitates reliable assignment of ³*J*_{H–H} values as large or small, the reduced resolution in the ¹³C dimension together with the smaller spread (0 to 6 Hz) of ^{2,3}*J*_{C–H} values makes even qualitative classification of long-range heteronuclear coupling constants more difficult and less reliable. As an

(14) Uhrin, D.; Batta, G.; Hruby, V. J.; Barlow, P. N.; Koeber, K. E. *J. Magn. Reson.* **1998**, *130*, 155.

(15) (a) Marquez, B. L.; Gerwick, W. H.; Williamson, R. T. *Magn. Reson. Chem.* **2001**, *39*, 499. (b) Williamson, R. T.; Marquez, B. L.; Gerwick, W. H.; Kover, K. E. *Magn. Reson. Chem.* **2000**, *38*, 265.

(16) Meissner, A.; Soerensen, O. W. *Magn. Reson. Chem.* **2001**, *39*, 49.

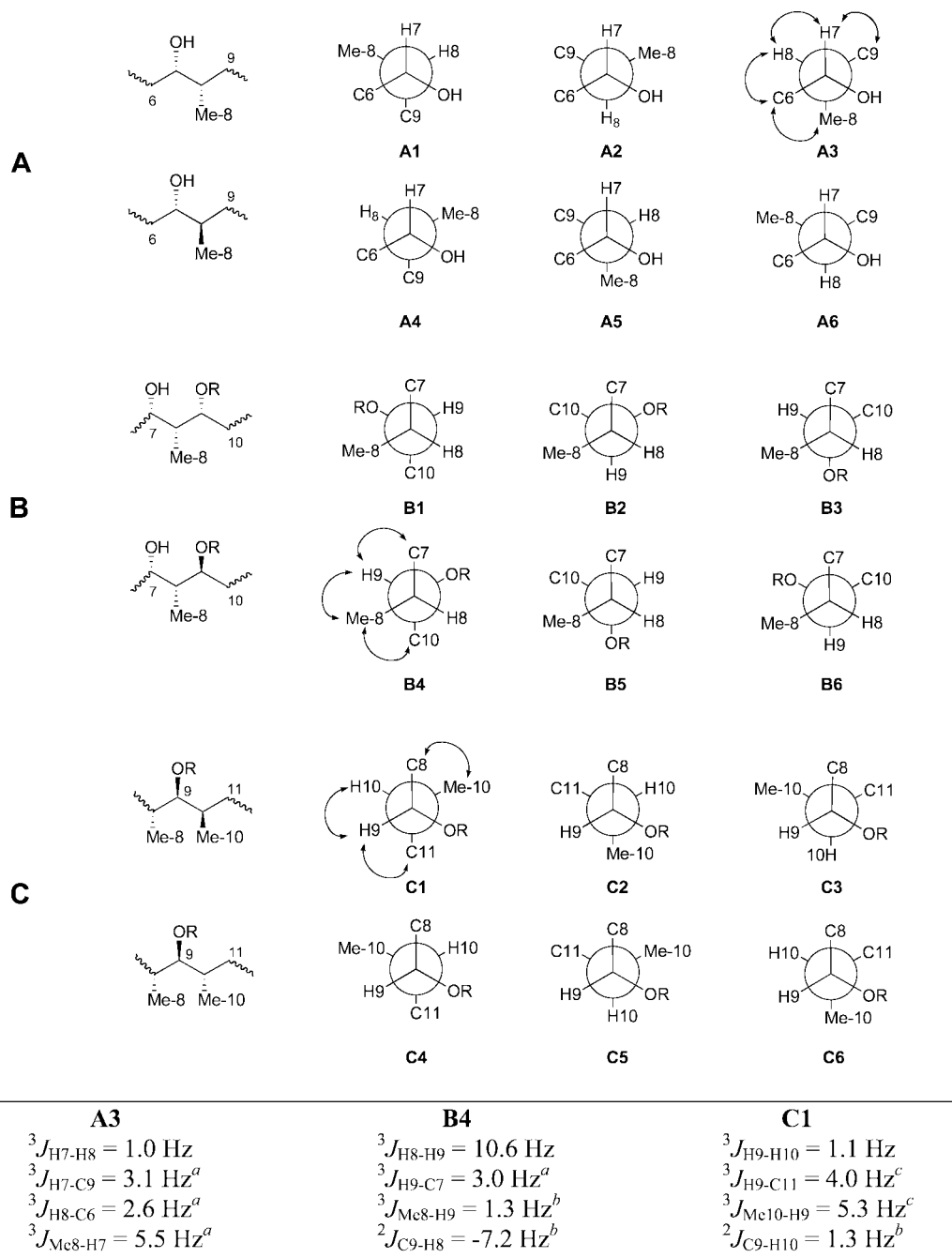
(17) Bax, A.; Davis, D. G. *J. Magn. Reson.* **1985**, *63*, 207.

(18) Bifulco, G.; Dambruoso, P.; Gomez-Paloma, L.; Riccio, R. *Chem. Rev.* **2007**, *107*, 3744.

(19) Bifulco, G.; Bassarello, C.; Riccio, R.; Gomez-Paloma, L. *Org. Lett.* **2004**, *6*, 1025–1028.

(12) Matsumori, N.; Kaneno, D.; Murata, M.; Nakamura, H.; Tachibana, K. *J. Org. Chem.* **1999**, *64*, 866.

(13) Griesinger, C.; Soerensen, O. W.; Ernst, R. R. *J. Magn. Reson.* **1987**, *75*, 474.



^a *J*-HMBC, ^b HETLOC, ^c HSQMBC

FIGURE 1. Newman projections showing all possible staggered rotamers for threo and erythro configurations viewed down bonds (A) C-7–C-8, (B) C-8–C-9, and (C) C-9–C-10 for the polyketide residue Dtdt in compound **1**. ${}^3J_{\text{H-H}}$ and ${}^{2,3}J_{\text{C-H}}$ values that led to the assignment of the rotamers **A3**, **B4**, and **C1** are displayed. Observed ROEs are shown as double-sided arrows.

example, experimental ${}^3J_{\text{C-H}}$ values for H-7/C-9, H-8/C-6, and H-9/C-11 within the Dtdt portion of **1** were found to be 3.1, 2.6, and 4.0 Hz, respectively, all of which may be classified as “medium”. To quantitatively compare experimental with predicted couplings surrounding these centers, we performed quantum mechanical calculations at the DFT MPW1PW91/6-31G(d,p) level of *J* values for all possible configurations in the simplified fragment **8** (represented by the stereoisomers shown in projections A1–A6, B1–B6, and C1–C6 in Figure 1). The results are summarized in Table 2 where the calculated values for the six possible conformers (three threo and three erythro arrangements) for stereocenter

pairs C-7/C-8, C-8/C-9, and C-9/C-10 are presented alongside their experimental values (far right column). Total absolute deviation (TAD) values, which provide an unbiased measure of the similarity between calculated and experimental coupling constants for each isomer, are shown in italics. Isomers displaying the lowest TAD values include A3 for C-7/C-8 (5.5 Hz), B4 for C-8/C-9 (5.5 Hz), and C1 for C-9/C-10 (4.2 Hz). These calculated values correspond to 7*S**, 8*R**, 9*S**, 10*R** configurations, confirming the *J*-based assignments presented above. It is noteworthy that, in addition to these configurations being self-consistent among stereocenter pairs, the results of the *J* coupling quantum chemical analysis are

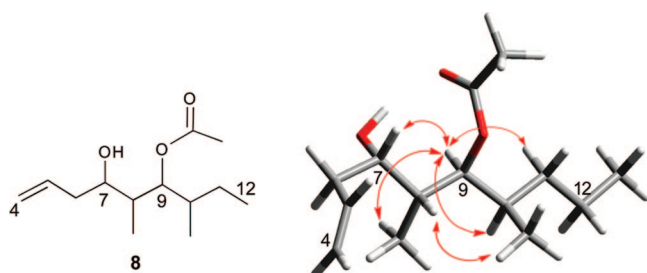
TABLE 2. Calculated and Experimental *J* Values for a Fragment Corresponding to Dddd in Celebeside A (1)

C-7/C-8	calculated ^a						experimental ^b
	threo			erythro			
	A1	A2	A3	A4	A5	A6	
H-7–Me-8	2.7	4.0	4.3	2.9	4.2	5.1	5.5
H-7–C-9	4.9	0.4	2.1	5.6	1.5	0.1	3.1
H-8–C-6	4.4	1.7	0.5	0.7	5.2	5.7	2.6
H-8–H-7	2.7	7.5	2.2	2.4	4.1	6.3	1.0
TAD ^c	8.0	11.7	5.5	8.4	8.7	11.8	

C-8/C-9	B1	B2	B3	B4	B5	B6	
H-8–C-9	–0.4	–4.8	–3.8	–4.1	–0.7	–5.2	–7.2
H-9–C-7	5.2	5.5	1.8	2.3	2.3	1.2	3.0
H-9–Me-8	1.5	3.6	2.7	1.0	6.5	5.1	1.3
H-9–H-8	2.0	2.5	9.0	9.2	1.2	5.1	10.6
TAD	17.8	15.3	7.6	5.5	21.9	13.0	

C9/C10	C1	C2	C3	C4	C5	C6	
H-9–Me-10	5.0	0.4	2.5	6.6	4.7	2.9	5.3
H-9–C-11	2.6	6.2	4.4	0.3	2.2	4.7	4.0
H-10–C-9	2.3	–2.0	–5.7	–2.1	–5.7	2.3	1.3
H-10–H-9	2.6	4.4	2.3	4.8	2.3	2.7	1.1
TAD	4.2	13.7	11.3	12.1	10.7	5.7	

^a *J* values calculated using DFT at the MPW1PW91/6-31G(d,p) level using Gaussian03.²⁰ ^b Experimental values derived from HMBC, HETLOC, and HSQMC spectra. ^c Total absolute deviation (TAD) values calculated using the equation ($\sum J_{\text{calc}} - J_{\text{exp}}$). Stereoisomers displaying the lowest TAD values appear in bold.

**FIGURE 2.** Chemical structure of **8**, representative of the C-4 to C-12 fragment of Dddd in **1–3**, and DFT mPW1PW91/6-31G(d,p) geometry and energy-optimized conformer. Observed ROEs are indicated with double-sided red arrows.

perfectly compatible with the experimental ROESY correlations (Figure 2).

Residues similar to Dddd have been found in the antibacterial depsipeptide nagahamide A²¹ and the antifungal antibiotic YM-47522.²² In both compounds the relative configuration of the polyketide residue was established as 7*R**, 8*R**, 9*S**, 10*R**, while the absolute configuration of YM-47522 was established as

(20) Gaussian 03, Revision B.05: Frisch, M. J.; Trucks, G. W.; Schlegel, H. B.; Scuseria, G. E.; Robb, M. A.; Cheeseman, J. R.; Montgomery, J. A., Jr.; Vreven, T.; Kudin, K. N.; Burant, J. C.; Millam, J. M.; Iyengar, S. S.; Tomasi, J.; Barone, V.; Mennucci, B.; Cossi, M.; Scalmani, G.; Rega, N.; Petersson, G. A.; Nakatsuji, H.; Hada, M.; Ehara, M.; Toyota, K.; Fukuda, R.; Hasegawa, J.; Ishida, M.; Nakajima, T.; Honda, Y.; Kitao, O.; Nakai, H.; Klene, M.; Li, X.; Knox, J. E.; Hratchian, H. P.; Cross, J. B.; Bakken, V.; Adamo, C.; Jaramillo, J.; Gomperts, R.; Stratmann, R. E.; Yazyev, O.; Austin, A. J.; Cammi, R.; Pomelli, C.; Ochterski, J. W.; Ayala, P. Y.; Morokuma, K.; Voth, G. A.; Salvador, P.; Dannenberg, J. J.; Zakrzewski, V. G.; Dapprich, S.; Daniels, A. D.; Strain, M. C.; Farkas, O.; Malick, D. K.; Rabuck, A. D.; Raghavachari, K.; Foresman, J. B.; Ortiz, J. V.; Cui, Q.; Baboul, A. G.; Clifford, S.; Cioslowski, J.; Stefanov, B. B.; Liu, G.; Liashenko, A.; Piskorz, P.; Komaromi, I.; Martin, R. L.; Fox, D. J.; Keith, T.; Al-Laham, M. A.; Peng, C. Y.; Nanayakkara, A.; Challacombe, M.; Gill, P. M. W.; Johnson, B.; Chen, W.; Wong, M. W.; Gonzalez, C.; Pople, J. A. Gaussian, Inc., Wallingford, CT, 2004.

(21) Okada, Y.; Matsunaga, S.; van Soest, R. W. M.; Fusetani, N. *Org. Lett.* **2002**, *4*, 3029.

7*S*, 8*S*, 9*R*, 10*S* by synthesis of its enantiomer.²³ In keeping with the different relative configurations at C-7 in celebeside A (7*S**) and nagahamide (7*R**), it is noteworthy that the ¹³C chemical shifts for Me10_{Dddd} in DMSO-*d*₆ differ significantly with respective δ_{C} values of 12.9 and 16.8.

The HR-ESI-MS of celebeside B (**2**) showed a major ion peak at *m/z* 878.3964 [M + H]⁺ (C₃₇H₆₀N₇O₁₆P, calcd for C₃₆H₆₁N₇O₁₆P, 878.3912), 14 mass units lower than that of **1**. The 2D NMR data for **2** closely resembled those of **1** with the exception that resonances belonging to the polyketide residue Dddd were replaced by resonances belonging to a 7,9-dihydroxy-8,10-dimethyldodeca-2,4-dienoic acid (Dddd) residue. HR-ESI-MS data gave a molecular formula C₃₇H₆₁N₇O₁₃ (*m/z* 812.4443 [M + H]⁺, calcd for C₃₇H₆₂N₇O₁₃, 812.4406) for celebeside C (**3**), 80 mass units below that of **1**. Analysis of the NMR data (¹H, ¹³C, HSQC, HMBC, DQF-COSY, 2D-HOHAHA) established **3** to be the dephosphorylated analogue of **1**. LC-MS analysis of the L/D-FDLA-derivatized hydrolysates of **2** and **3** revealed all amino acid residues to possess configurations identical to those in **1**. Additionally, analysis of the NMR data corresponding to signals belonging to the polyketide unit indicated that the configurations in **2** and **3** are the same as those in **1**.

Evident from the mass spectral data, Sephadex fractions containing the celebesides also contained a suite of compounds with considerably higher masses. The molecular formula of **4** was established as C₇₁H₁₂₅N₁₇O₂₄ on the basis of HR-ESI-MS (*m/z* 800.9600 [M + 2H]²⁺, calcd for C₇₁H₁₂₅N₁₇O₂₄, 1599.9083). Its NMR spectrum displayed characteristic signals of a peptide, including resonances attributable to exchangeable amide protons between δ 9.16 and 6.20, α -amino protons between δ 5.12 and 3.90, two methyl amide signals at δ 2.82 (3H, s) and 2.86 (3H, s), and one ester carbinol proton at δ 5.12 (1H, d, *J* = 3.6 Hz). Additionally, the ¹H NMR spectrum showed signals corresponding to a methoxyl at δ 3.34 (3H, s), an acetamide methyl at δ 1.90 (3H, s), and a primary methyl at δ 0.83 (3H, t, *J* = 7.3 Hz). A detailed analysis of the 2D NMR data established the presence of one equivalent each of *N*-methylleucine (*N*MeLeu), asparagine, β -methoxyasparagine (β -OMeAsn), *N*-methylglutamine (*N*MeGlu), leucine, ornithine, 3,4-dimethylglutamine (3,4-DiMeGln), 3-hydroxy-2,4,6-trimethyloctanoic acid (Htoa), and two threonine residues, one of which was *O*-acylated. The presence of an unusual 3-acetamido-2-amino-propanoic acid (Acpa) was established by HMBC correlations from the β -aminomethylene protons at δ 3.54 and 3.49 to the acetamide carbonyl at δ 174.9. The presence of 4-amino-2,3,5-trihydroxy-5-methylhexanoic acid (Amtha) was deduced as follows. A contiguous spin system comprising two oxymethine signals (δ_{H} 3.75, δ_{C} 71.8 and δ_{H} 4.06, δ_{C} 71.5) and one aminomethine signal (δ_{H} 3.97, δ_{C} 56.1) was apparent from HSQC, COSY and TOCSY spectra. HMBC correlations from the oxymethine proton at δ 3.75 to the carbonyl resonance at δ 176.9 (C-1_{Amtha}); and from the methyl protons at δ 1.24 (Me-6_{Amtha}) and 1.09 (Me-5_{Amtha}), and the aminomethine proton at δ 3.97, to the oxygenated quaternary carbon at 74.9 (C-4_{Amtha}) secured the structure of this residue.

Long-range correlations between α -protons and carbonyl carbons of adjacent amino acids provided the sequence (in the

(22) (a) Shibazaki, M.; Sugawara, T.; Nagai, K.; Shimizu, Y.; Yamaguchi, H.; Suzuki, K. *J. Antibiot.* **1996**, *49*, 340. (b) Sugawara, T.; Shibazaki, M.; Nakahara, H.; Suzuki, K. *J. Antibiot.* **1996**, *49*, 345.

(23) Ermolenko, M. S. *Tetrahedron Lett.* **1996**, *37*, 6711.

direction CO to N) *N*MeLeu-Asn- β -OMeAsn-*N*MeGlu-Leu-Orn-Thr1-Thr2-3,4-DiMeGln-Amtha for **4**, with the hydroxyl group of Thr2 forming an ester bond with the carboxyl group of *N*MeLeu. The remainder of the sequence was deduced from HMBC spectra. In particular, long-range correlations between the aminomethine proton H-4_{Amtha} and the carbonyl resonance at δ 173.1 (C-1_{Acpa}) linked Acpa to the main fragment, while an HMBC correlation between the α -proton at δ 4.49 (H-2_{Acpa}) and the carbonyl resonance at δ 179.4 (C-1_{Htoa}), linked the fatty acid Htoa to Acpa. This sequence was further corroborated by analysis of the MS/MS spectrum. Fragmentation of the doubly charged ion peak at *m/z* 801 [M + 2H]²⁺ displayed fragment ions at *m/z* 1271 [M + H-Htoa-Acpa-NH₃]⁺, *m/z* 957 [M + H-Htoa-Acpa-Amtha-3,4-DiMeGln]⁺, *m/z* 754 [M + H-Htoa-Acpa-Amtha-3,4-DiMeGln-Thr-Thr]⁺, and *m/z* 627 [M + H-Htoa-Acpa-Amtha-3,4-DiMeGln-Thr-Thr-*N*MeLeu]⁺, consistent with the sequence established for **4**.

The absolute configurations of *L*-*N*MeLeu, *L*-*N*MeGln, *L*-Leu, *D*-Orn, *D*-allo-Thr, and *D*-Acpa were assigned by chromatographic comparison of the acid hydrolysate of **4** (5 *N* HCl, 90 °C, 16 h) with appropriate amino acid standards after derivatizing with *L/D*-FDLA (1-fluoro-2,4-dinitrophenyl-5-*L/D*-leucinamide).⁹ Comparison by LC-MS of the *L/D*-FDLA derivative of 3,4-DiMeGln of **4** with that derivative from the hydrolysate of an authentic sample of mirabamide A⁷ showed that DiMeGln has the same configuration, (3*S*,4*R*)-dimethyl-*L*-glutamine, in both peptides. Chiral HPLC following acid hydrolysis of **4** established the *D* configuration for Asn.

The HR-ESI-MS of **5** and **6** showed doubly charged ion peaks at *m/z* 792.9615 [M + 2H]²⁺ and *m/z* 799.9722 [M + 2H]²⁺ corresponding to molecular formulas of C₇₁H₁₂₅N₁₇O₂₃ (calcd for C₇₁H₁₂₅N₁₇O₂₃, 1583.9134) and C₇₂H₁₂₇N₁₇O₂₃ (calcd for C₇₂H₁₂₇N₁₇O₂₃, 1597.9291), respectively. These values indicated that the molecular weight of **5** was 16 mu lower than **4** while **6** was 14 mu higher than **5**. A detailed analysis of the NMR data of **5** clearly established that its amino acid sequence was identical to **4**, except for the occurrence of a 4-amino-2,3-dihydroxy-5-methylhexanoic acid (Amdha) residue instead of Amtha. Similarly, the 2D NMR data of **6** differed to that of **5** by the substitution of an uncommon homoisoleucine (hIle) residue for a leucine residue. Once again, LC-MS analysis of the *L/D*-FDLA-derivatized hydrolysates of **5** and **6** revealed that all the amino acid residues possessed identical configurations to that in **4**, and the configuration of hIle was established as *L*.

On the basis of the amino acid sequences of **4**–**6**, it was evident that these depsipeptides resembled theopapuamide (**7**), previously isolated from an extract of *T. swinhoei* Gray collected in Papua New Guinea, and reported to be cytotoxic.⁸ However, the configuration of the chiral centers in the polyketide residues in theopapuamide were not reported.

In theopapuamide B (**4**), the relative configurations of the chiral centers C-3/C-4 in Amtha, and C-2/C-3 in Htoa were solved using again *J*-based configuration analysis in the following manner. A large ³*J*_{H-H} of 9.1 Hz obtained from the phase-sensitive COSY-35 spectrum²⁴ indicated an anti orientation between protons H-2_{Htoa} and H-3_{Htoa} (Figure 3a). The anti configuration between Me-2_{Htoa} and the hydroxyl group at C-3_{Htoa} was assigned on the basis of ROESY correlations between Me-2_{Htoa}/H-4_{Htoa}, Me-2_{Htoa}/H-3_{Htoa}, and H-2_{Htoa}/H-4_{Htoa}. The configuration at C-3_{Htoa}/C-4_{Htoa}, however, could not be solved using the *J*-based analysis because of alternation between

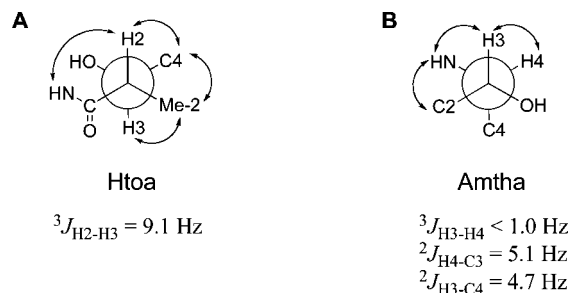


FIGURE 3. Newman projections, ³*J*_{H-H} and ^{2,3}*J*_{C-H} values, and ROESY correlations used to establish the relative configurations of A) C-2/C-3 in Htoa, and B) C-3/C-4 in Amtha.

TABLE 3. Biological Activities

compd	HIV-1 neutralization	HCT-116
1	1.9 ± 0.4	8.8 ± 3.0
3	>50	>25
4	0.8 ± 0.3	2.1 ± 0.7
5	nt	4.0 ± 1.7
7	nt	2.1 ± 0.9

conformers.¹³ This situation was apparent from the small ³*J*_{H-H} between H-3_{Htoa} and H-4_{Htoa} (2.3 Hz), and intermediate ³*J*_{C-H} values of 4.6 and 4.5 Hz between H-3_{Htoa} and C-5_{Htoa}, and H-3_{Htoa} and Me-4_{Htoa}, respectively, indicating alternation between *g*⁺ and *g*⁻ conformers at C-3/C-4. Recently, Zampella et al. reported the structure of homophymine, a cyclic depsipeptide that also contains an exocyclic Htoa residue (referred to in that paper as HTMOA).²⁵ In the case of homophymine, the authors did not report conformational averaging around C-3/C-4, and through the combined use of *J*-based, NOE, and Mosher's analysis were able to assign a 2*R*,3*R*,4*R*,6*R* configuration for that residue.

Within the Amtha residue, a small ³*J*_{H-H} (<1 Hz) between H-3_{Amtha} and H-4_{Amtha} suggested a gauche orientation between these two protons (Figure 3b). Moreover, the constant time *J*-resolved HMBC spectrum showed large ²*J*_{C-H} coupling constants of 5.1 and 4.7 Hz between H-4_{Amtha} and C-3_{Amtha} and between H-3_{Amtha} and C-4_{Amtha}, respectively. Together these values indicated a syn configuration at C-3_{Amtha}/C-4_{Amtha}. Within the β -OMeAsn residue, however, alternation between *g*⁺ and *g*⁻ conformers at C-2/C-3, apparent from small ³*J*_{H-H} and intermediate ²*J*_{C-H} values, precluded our ability to use these methods to establish its relative configuration. Last, analysis of the NMR data of the polyketide residues Htoa and Amdha in theopapuamides C and D suggested identical relative configurations to those observed for theopapuamide B.

Celebesides A and C and theopapuamides A–C were evaluated in a single round HIV-1 infectivity assay^{26,27} against viruses pseudotyped with HIV-1 SF162 Envelope, and a cytotoxicity assay using human colon tumor cell line HCT-116. The results are summarized in Table 3. Interestingly, celebeside A inhibits HIV-1 Entry with an IC₅₀ value of 1.9 ± 0.4 μ g/mL, while the nonphosphorylated celebeside C was inactive at

(25) Zampella, A.; Sepe, V.; Luciano, P.; Bellotta, F.; Monti, M. C.; D'Auria, M. V.; Jepsen, T.; Petek, S.; Adeline, M.-T.; Laprévôte, O.; Aubertin, A.-M.; Debitus, C.; Poupat, C.; Ahond, A. *J. Org. Chem.* **2008**, *73*, 5319.

(26) Li, M.; Gao, F.; Mascola, J. R.; Stamatatos, L.; Polonis, V. R.; Koutsoukos, M.; Voss, G.; Goepfert, P.; Gilbert, P.; Greene, K. M.; Bilksa, M.; Kothe, D. L.; Salazar-Gonzalez, J. F.; Wei, X.; Decker, J. M.; Hahn, B. H.; Montefiori, D. C. *J. Virol.* **2005**, *79*, 10108.

(27) Gustchina, E.; Bewley, C. A.; Clore, G. M. *J. Virol.* **2008**, in press; PMID 18667502.

(24) Bax, A.; Freeman, R. *J. Magn. Reson.* **1981**, *44*, 542.

concentrations as high as 50 $\mu\text{g/mL}$. Theopapuamide B (**4**) was active in the neutralization assay with an IC_{50} value of $0.8 \pm 0.3 \mu\text{g/mL}$; however, we found theopapuamides A–C to be cytotoxic to other healthy cell lines at similar concentrations (data not shown). Celebeside A and theopapuamides A–C were also cytotoxic to a human colon tumor cell line (HCT-116) with IC_{50} values of 8.8, 2.1, 4.0, and 2.1 $\mu\text{g/mL}$, respectively.

The antifungal activity of the crude extract was traced to the theopapuamides, and testing of pure compounds **4–7** revealed activity against both wild type and amphotericin B-resistant strains of *Candida albicans*. In particular, theopapuamide A inhibited growth of wild type and amphotericin B-resistant strains at loadings of 1 $\mu\text{g/disk}$, displaying zones of growth inhibition of 8 mm; and theopapuamides B and C were slightly less potent, displaying zones of inhibition of 10 mm at 5 $\mu\text{g/disk}$ against both strains. All three celebesides were found to be inactive toward *Bacillus subtilis*, *Escherichia coli*, *Pseudomonas aeruginosa*, *Staphylococcus aureus*, and *C. albicans* at concentrations as high as 50 $\mu\text{g/disk}$.

In summary, we have isolated six new depsipeptides from an *S. mirabilis* sponge collected from Indonesia. Celebesides A–C (**1–3**) are cyclic depsipeptides that contain the polyketide moiety Dtd and five amino acid residues, among which are the unusual amino acids phosphoserine and 3-carbamoyl threonine, both of which are new to marine natural products. Interestingly, the anti-HIV activity of celebesides correlates with the presence of phosphoserine. The undecapeptides theopapuamides B–D (**4–6**) are further members of the theopapuamide class reported recently by Ireland and co-workers. Theopapuamides C and D contain two new entities, including 3-acetamido-2-aminopropanoic acid and 4-amino-2,3-dihydroxy-5-methylhexanoic acid, while theopapuamide D contains a rare homoisoleucine residue. Theopapuamides A–C showed strong antifungal activity toward amphotericin B-resistant *C. albicans* and its parent strain. Thus, celebesides and theopapuamides represent interesting new classes of anti-infectives. In addition to these six new depsipeptides, aurantosides A and B²⁸ and keramamide A²⁹ were also found in the aqueous extract of this sponge. The presence of this suite of compounds in a single collection of *S. mirabilis* further emphasizes the chemical diversity present in lithistid demosponges.

Experimental Section

General Experimental Procedures. Optical rotations were measured with a JASCO P-2000 polarimeter, IR spectra were recorded on a Perkin-Elmer FT-IR Spectrum One spectrometer, and UV spectra were recorded on an Agilent 8453 spectrophotometer. NMR spectra were recorded in 5:1 or 4:1 $\text{CD}_3\text{CN}-\text{H}_2\text{O}$ on a Bruker DRX-600 spectrometer (^1H at 600 MHz, ^{13}C at 150 MHz). DQF-COSY, 2D-HOHAHA, HSQC, HMBC, and ROESY experiments were recorded using standard pulse programs, all of which included water suppression (Watergate). HSQC experiments were optimized for $^1J_{\text{C-H}} = 145 \text{ Hz}$, and HMBC spectra were optimized for $^2,3J_{\text{C-H}} = 8$ and 5 Hz. The accurate mass electrospray ionization (ESI) mass spectra were measured on a Waters LCT Premier time-of-flight (TOF) mass spectrometer. The instrument was operated in W-mode at a nominal resolution of 10000. The electrospray capillary voltage was set at 2 kV and the sample cone voltage at 60 V. The desolvation temperature was set to 275 $^\circ\text{C}$, and nitrogen

was used as the desolvation gas with a flow rate of 300 L/hr. Accurate masses were obtained using the internal reference standard method. MS/MS data were obtained using a Thermo-Scientific (San Jose, CA) LTQ ion Trap mass spectrometer. Sample was infused into the mass spectrometer using an Advion BioSciences (Ithaca, NY) Triversa chip based nanoelectrospray ionization system. The nitrogen gas pressure was 0.25 psi, and the electrospray tip voltage was 1.4 kV. The CID MS/MS collision energy was 35 V, and the parent ion isolation width was 3 Da. The maximum injection time for parent ions was 700 and 500 ms for daughter ions. The maximum AGC ion target setting was 1×10^5 for parent ions and 5×10^4 for daughter ions.

Computational Details. For the quantum mechanical calculations, both full geometry optimization and calculation of J -coupling values were performed using the Gaussian03 (version B.05) software package.²⁰ The gauche- or anti-staggered conformers of a simplified fragment, **8**, containing 14 carbon atoms were optimized at mPW1PW91 level of theory using the 6-31G(d,p) basis set; the single-point calculation of J -coupling was executed on the optimized geometries using the same mPW1PW91 functional and the 6-31G(d,p) basis set.

Sponge Material. Samples of *S. mirabilis* (deLaubenfels, 1954) (lithistid Demospongiae: family Theonellidae) were collected around Sulawesi Island, Indonesia, at a depth of 43 m in 1994. The sample was identified as described previously,⁶ and a voucher specimen has been deposited at the Natural History Museum, London (BMNH 2007.7.9.1). Samples were frozen immediately after collection and shipped frozen to Frederick, MD, where they were freeze-dried and extracted with H_2O .

Isolation. A 6 g portion of the extract was partitioned between $n\text{-BuOH}-\text{H}_2\text{O}$ (1:1) to afford a dried $n\text{-BuOH}$ extract (0.7 g) that was fractionated on a Sephadex LH-20 column ($50 \times 2.5 \text{ cm}$) eluting with $\text{MeOH}/\text{H}_2\text{O}$ (7:3). Fractions containing peptides were combined and dried in vacuo to give 130 mg that were subsequently purified by reverse-phase HPLC (Jupiter Proteo C12, $250 \times 10 \text{ mm}$, 4 μm , DAD at 220 and 280 nm) eluting with a linear gradient of 50–80% MeOH in 0.05% TFA in 50 min to afford compounds **1** (7.2 mg, $t_{\text{R}} = 43.9 \text{ min}$), **2** (2.4 mg, $t_{\text{R}} = 34.9 \text{ min}$), **3** (1.1 mg, $t_{\text{R}} = 40.0 \text{ min}$), **4** (2.5 mg, $t_{\text{R}} = 32.9 \text{ min}$), **5** (1.8 mg, $t_{\text{R}} = 33.5 \text{ min}$), **6** (0.8 mg, $t_{\text{R}} = 36.8 \text{ min}$), and **7** (3.4 mg, $t_{\text{R}} = 24.3 \text{ min}$).

Celebeside A (1): Colorless amorphous powder; $[\alpha]_{\text{D}}^{23} -49.9$ (c 0.32, MeOH); IR (film) ν_{max} 3333, 1665, 1534, 1201, 1139, 1076 cm^{-1} ; UV (MeOH) λ_{max} ($\log \epsilon$) 210 (2.98), 270 (2.17) nm; ^1H and ^{13}C NMR data, see Table 1; HR-ESI-MS m/z 892.4054 $[\text{M} + \text{H}]^+$ corresponding to a molecular formula of $\text{C}_{37}\text{H}_{63}\text{N}_7\text{O}_{16}\text{P}$ (calcd for $\text{C}_{37}\text{H}_{63}\text{N}_7\text{O}_{16}\text{P}$, 892.40689).

Celebeside B (2): Colorless amorphous powder; $[\alpha]_{\text{D}}^{23} -2.0$ (c 0.05, MeOH); IR (film) ν_{max} 3330, 1663, 1538, 1207, 1132, 1075 cm^{-1} ; UV (MeOH) λ_{max} ($\log \epsilon$) 210 (2.96), 271 (2.15) nm; ^1H and ^{13}C NMR data for Iser, Thr, βMeAsn , pSer, and NMeVal are identical to those reported for **1** in Table 1; ^1H NMR ($\text{CD}_3\text{CN}-\text{H}_2\text{O}$ 5:1, 600 MHz) Dddd: δ 6.02 (1H, d, $J = 15.5 \text{ Hz}$, H-2), 7.05 (1H, dd, $J = 15.5, 11.1 \text{ Hz}$, H-3), 6.25 (1H, dd, $J = 15.3, 11.1 \text{ Hz}$, H-4), 6.01 (1H, dd, $J = 15.3, 6.6 \text{ Hz}$, H-5), 2.40 (1H, td, $J = 13.9, 6.6 \text{ Hz}$, H-6a), 2.22 (1H, td, $J = 13.9, 6.5 \text{ Hz}$, H-6b), 3.36 (1H, t, $J = 7.4 \text{ Hz}$, H-7), 1.70 (1H, m, H-8), 5.04 (1H, dd, $J = 10.6, 1.1 \text{ Hz}$, H-9), 1.64 (1H, m, H-10), 1.25 (1H, m, H-11a), 1.11 (1H, m, H-11b), 0.87 (3H, t, $J = 7.0 \text{ Hz}$, Me-12), 0.78 (3H, d, $J = 7.0 \text{ Hz}$, Me-8), 0.79 (3H, d, $J = 6.3 \text{ Hz}$, Me-10); ^{13}C NMR ($\text{CD}_3\text{CN}-\text{H}_2\text{O}$ 5:1, 150 MHz) Dddd: δ 169.5 (C-1), 123.5 (C-2), 141.6 (C-3), 131.8 (C-4), 140.3 (C-5), 39.0 (C-6), 70.6 (C-7), 38.5 (C-8), 78.6 (C-9), 37.0 (C-10), 28.2 (C-11), 12.4 (Me-12), 9.3 (Me-8), 13.0 (Me-10); HR-ESI-MS m/z 878.3964 $[\text{M} + \text{H}]^+$ ($\text{C}_{37}\text{H}_{60}\text{N}_7\text{O}_{16}\text{P}$, calcd for $\text{C}_{36}\text{H}_{61}\text{N}_7\text{O}_{16}\text{P}$, 878.3912).

Celebeside C (3): Colorless amorphous powder; $[\alpha]_{\text{D}}^{23} -3.4$ (c 0.06, MeOH); IR (film) ν_{max} 3420, 1676, 1192, 1130 cm^{-1} ; UV (MeOH); λ_{max} ($\log \epsilon$) 211 (2.98), 272 (2.17) nm; ^1H and ^{13}C NMR data for Iser, Thr, βMeAsn , NMeVal, and Dtd are identical to those reported for **1** in Table 1; ^1H NMR ($\text{CD}_3\text{CN}-\text{H}_2\text{O}$ 5:1, 600 MHz)

(28) Matsunaga, S.; Fusetani, N.; Kato, Y. *J. Am. Chem. Soc.* **1991**, *113*, 9690–9692.

(29) Kobayashi, J.; Sato, M.; Ishibashi, M.; Shigemori, H.; Nakamura, T.; Ohizumi, Y. *J. Chem. Soc., Perkin Trans. 1* **1991**, 1050–1052.

Ser: δ 4.78 (1H, m, H-2), 3.54 (1H, m, H-3a), 3.50 (1H, m, H-3b), 7.61 (1H, br, NH); ^{13}C NMR ($\text{CD}_3\text{CN}-\text{H}_2\text{O}$ 5:1, 150 MHz) Ser: δ 171.2 (C-1), 53.3 (C-2); HR-ESI-MS m/z 812.4443 $[\text{M} + \text{H}]^+$ ($\text{C}_{37}\text{H}_{61}\text{N}_7\text{O}_{13}$, calcd for $\text{C}_{37}\text{H}_{62}\text{N}_7\text{O}_{13}$, 812.4406)

Theopapuamide B (4): Colorless amorphous powder; $[\alpha]_D^{23}$ 7.1 (c 0.1, MeOH); IR (film) ν_{max} 3329, 1673, 1536, 1205, 1185, 1138 cm^{-1} ; UV (MeOH) λ_{max} (log ϵ) 210 (3.84) nm; HR-ESI-MS m/z 800.9600 $[\text{M} + 2\text{H}]^{2+}$, (calcd for $\text{C}_{71}\text{H}_{125}\text{N}_{17}\text{O}_{24}$, 1599.9083). See the Supporting Information for ^1H and ^{13}C NMR assignments.

Theopapuamide C (5): Colorless amorphous powder; $[\alpha]_D^{23}$ 5.1 (c 0.08, MeOH); IR (film) ν_{max} 3319, 1673, 1534, 1203, 1181, 1134 cm^{-1} ; UV (MeOH) λ_{max} (log ϵ) 210 (3.83) nm; HR-ESI-MS m/z 792.9615 $[\text{M} + 2\text{H}]^{2+}$, (calcd for $\text{C}_{71}\text{H}_{125}\text{N}_{17}\text{O}_{23}$, 1583.9134). See the Supporting Information for ^1H and ^{13}C NMR assignments.

Theopapuamide D (6): Colorless amorphous powder; $[\alpha]_D^{23}$ 2.5 (c 0.03, MeOH); IR (film) ν_{max} 3325, 1675, 1532, 1208, 1185, 1139 cm^{-1} ; UV (MeOH) λ_{max} (log ϵ) 210 (3.84) nm; HR-ESI-MS m/z 799.9722 $[\text{M} + 2\text{H}]^{2+}$, (calcd for $\text{C}_{72}\text{H}_{127}\text{N}_{17}\text{O}_{23}$, 1597.9291). See the Supporting Information for ^1H and ^{13}C NMR assignments.

Theopapuamide A (7): Colorless amorphous powder; $[\alpha]_D^{23}$ 6.4 (c 0.2, MeOH); HR-ESI-MS m/z 779.9548 $[\text{M} + 2\text{H}]^{2+}$, (calcd for $\text{C}_{69}\text{H}_{123}\text{N}_{17}\text{O}_{23}$, 1557.8978).

LC/MS Analysis of L/D-FDLA Derivatives. Approximately 0.5 mg of compounds **1–6** was separately hydrolyzed with 5 N HCl (LabChem, Inc., traceable to NIST) (0.8 mL) in an Ace high pressure tube for 16 h at 90 °C, dried, and dissolved in H_2O (100 μL). To a 50 μL aliquot of each were added 1 N NaHCO_3 (20 μL) and 1% 1-fluoro-2,4-dinitrophenyl-5-L-leucinamide (L-FDLA or D-FDLA solution in acetone, 100 μL), and the mixtures were heated to 40 °C for 40 min, allowed to cool to rt, neutralized with 2 N HCl (20 μL), and evaporated to dryness. Residues were dissolved in CH_3CN and analyzed by LC–MS. Analyses of the L- and L/D-FDLA (mixture of D- and L-FDLA) derivatives were performed using a Phenomenex Jupiter Proteo C12 column (4 μm , 150 \times 4.6 mm). Aqueous CH_3CN containing 0.01% TFA was used as a mobile phase eluting with a linear gradient of 25–70% CH_3CN in 45 min at a flow rate of 0.5 mL/min. An Agilent Series 1100 MSD mass spectrometer was used for detection in negative ESI mode. The fragmentor and capillary voltage were kept at 70 and 1000 V, respectively, and the ion source at 350 °C. A mass range of m/z 100–1000 was scanned in 0.1 min. Retention times (t_R , min) of the FDLA-derivatized amino acids for compounds **1–3**: L-Iser 19.9, D-Iser 19.3 m/z 398 $[\text{M} - \text{H}]^-$; L-NMeVal 29.7, D-NMeVal 33.2 m/z 424 $[\text{M} - \text{H}]^-$; L-Thr 19.3, D-Thr 23.2 m/z 412 $[\text{M} - \text{H}]^-$; erythro-L- β MeAsn 20.8, erythro-D- β MeAsn 24.1 m/z 440 $[\text{M} - \text{H}]^-$. Retention times (t_R , min) of the FDLA-derivatized amino acids for compounds **4–6**: L-NMeLeu 33.5, D-NMeLeu 35.5 m/z 438 $[\text{M} - \text{H}]^-$; L-NMeGln 19.7, D-NMeGln 21.0 m/z 426 $[\text{M} - \text{H}]^-$; L-Leu 30.6, D-Leu 36.6 m/z 424 $[\text{M} - \text{H}]^-$; L-Orn 36.8, D-Orn 34.8 m/z 720 $[\text{M} - \text{H}]^-$ (bis derivative); L-*allo*Thr 20.5, D-*allo*Thr 21.8 m/z 412 $[\text{M} - \text{H}]^-$; (3*S*,4*R*)-dimethyl-L-glutamine 23.3, (3*S*,4*R*)-dimethyl-D-glutamine 24.3 m/z 467 $[\text{M} - \text{H}]^-$; L-Dpa 37.5, D-Dpa 38.0 m/z 692 $[\text{M} - \text{H}]^-$ (bis derivative); L-hlle 30.1, D-hlle 39.3 m/z 438 $[\text{M} - \text{H}]^-$.

Chiral HPLC Analysis. The acid hydrosylates of **3–6** (0.3 mg) were analyzed by chiral HPLC on a Phenomenex column [Chirex phase 3126 (D) 150 \times 4.6 mm] eluting with 1 mM $\text{CuSO}_4/\text{MeCN}$ (95:5) at a flow rate of 0.5 mL/min, with UV detection at 254. The retention times of Asp were compared to authentic standards whose retention times were 15.5 min for L-Asp and 19.9 min for D-Asp.

Biological Assays. Cytotoxicity assays were carried out using an MTT cell proliferation assay kit (American type Culture Collection) according to the instructions provided. Briefly, HCT-116 or TZM-BL cells were seeded in 96-well tissue culture plates at a density of 2×10^4 cells/well in 50 μL of growth media and allowed to adhere for 18 h. Attached cells were incubated with inhibitors for 24 h (as controls for the neutralization assay), after which the media was either replaced or diluted 3-fold with fresh growth media. Following an additional 48 h incubation period, cell viability was assessed upon treatment with MTT (A_{570} , Molecular Devices 96-well absorbance plate reader). Single round HIV-1 neutralization assays were performed with viruses pseudotyped with SF162 Envelope using published conditions.²⁶

Antimicrobial Activity. Compounds **1–6** were tested for antimicrobial activity against *P. aeruginosa* (ATCC 15442), *E. coli* (ATCC 8739), *S. aureus* (ATCC 25923), *B. subtilis* (ATCC 49343), and wild type (ATCC 90027) and amphotericin B resistant *C. albicans* (ATCC 200955) using a modified disk diffusion assay. Agar plates seeded with suspensions of bacteria or fungi were prepared by adding 500 μL of a 24 h culture of bacteria to 100 mL of autoclaved Antibiotic Medium 2 (AB2) containing 1% agar and cooled to 55 °C, or of fungi to Sabouraud Dextrose Agar (SDA) at 55 °C. Seeded liquid agar (10 mL) was transferred immediately to square Petri dishes and allowed to cool for 1 h. Control drugs used for each microorganism included kanamycin (50 μg) for *P. aeruginosa* and *S. aureus*, ampicillin (50 μg) for *E. coli*, chloroamphenicol (10 μg) for *B. subtilis*, and amphotericin B (25 μg) for *C. albicans*. Following incubation at 37 °C for 18 h, zones of inhibition resulting from antibiotics or depsipeptides (1–50 μg) were measured.

Acknowledgment. We thank the Coral Reef Research Foundation, D. Newman, and the country of Indonesia for making possible sample acquisition; M. Kelly and the National Cancer Institute for sponge taxonomy; L. Bell, CRRF, for helpful discussions; and the AIDS Research and Reference Reagent Program, Division of AIDS, NIAID, NIH, for reagents and cell lines used in the HIV-1 neutralization assays. This work was supported in part by the NIH Intramural Research Program (NIDDK) and the Intramural AIDS Targeted Antiviral Program, Office of the Director, NIH (C.A.B.).

Supporting Information Available: Table of ^1H , and ^{13}C assignments for **4–6**, 1D and 2D (^1H , ^1H and ^1H , ^{13}C) NMR data used for structure elucidation of compounds **1–6**, and mass spectra for compounds **1** and **4**. This material is available free of charge via the Internet at <http://pubs.acs.org>.

JO802232U